

# Potassium Promotion of Cobalt Spinel Catalyst for N<sub>2</sub>O Decomposition—Accounted by Work Function Measurements and DFT Modelling

Filip Zasada · Pawel Stelmachowski ·  
Gabriela Maniak · Jean-Francois Paul ·  
Andrzej Kotarba · Zbigniew Sojka

Received: 4 July 2008 / Accepted: 9 September 2008 / Published online: 30 September 2008  
© Springer Science+Business Media, LLC 2008

**Abstract** The beneficial effect (decrease of the half conversion temperature by 100 °C) of potassium doping, in the range of 0–5 atoms/nm<sup>2</sup>, on N<sub>2</sub>O decomposition over Co<sub>3</sub>O<sub>4</sub> was analyzed by work function measurements and DFT calculations. The optimal potassium surface loading was found to be 1.8 atoms/nm<sup>2</sup>. The effect was explained in terms of electronic promotion gauged by lowering of the catalyst work function by 0.48 eV (for K<sub>2</sub>CO<sub>3</sub> precursor) and 0.44 eV (for KOH). The promotional effect is discussed in relation to the theoretical and experimental surface dipoles determined from Hirshfeld atomic charges and geometry of the postulated potassium adspecies and from the Topping model, respectively.

**Keywords** Cobalt spinel · Potassium promoter · N<sub>2</sub>O decomposition · Work function · Dipole moment · DFT

## 1 Introduction

Nitrous oxide is widely recognized as important greenhouse gas and the ozone layer destructor [1]. It is emitted from natural and anthropogenic sources and its concentration in the atmosphere is continuously increasing with the

annual growth rate of about 0.3% [1]. Because of the harmful effect to environment decomposition of N<sub>2</sub>O into N<sub>2</sub> and O<sub>2</sub> is a topic of vital interest for catalytic chemistry [1, 2]. Despite of its thermodynamic instability, N<sub>2</sub>O is kinetically inert toward direct decomposition into the constituting elements. Thus, this reaction, to be efficient, requires a catalyst for practical applications, especially in the excess of water and oxygen, usually present in the real conditions [2, 3]. However, none of the many catalysts developed until now exhibit satisfactory performance in real deN<sub>2</sub>O process, especially at low temperature regime (below 350 °C) such as those of tertiary abatement in nitric acid plants [3, 4]. So far, many catalytic systems such as noble metals [5, 6], metal oxides [7, 8], ion-exchanged zeolites [9, 10] were investigated for the low temperature deN<sub>2</sub>O, but the satisfactory solution in the presence of oxygen and water is still lacking. One of the simple promising systems exhibiting high catalytic activity in such reaction is cobalt spinel [11–13]. Modification by substitution with various transition or alkaline earth metal ions (such as Zn, Ni, Cu, Mn, Al, Mg,) leads to further improvement of the Co<sub>3</sub>O<sub>4</sub> catalyst activity [14–16]. Recently it has been found that doping of Co<sub>3</sub>O<sub>4</sub> with alkali has also a beneficial effect on the catalytic performance in deN<sub>2</sub>O reaction [11–13, 17].

Reported in the literature effect of Co<sub>3</sub>O<sub>4</sub> doping with alkali metals has not always been achieved intentionally [13], but resulted from the applied synthesis procedure, where potassium or sodium carbonates or hydroxides are commonly used as precipitating agents. As a result the residual alkali impurities may easily be entrapped in the cobalt hydroxycarbonate precursor of the spinel catalyst [18]. The effect of potassium was associated with enhanced reducibility of Co<sup>3+</sup> produced upon oxidation of Co<sup>2+</sup> during N<sub>2</sub>O decomposition. This redox conjecture has been

F. Zasada · P. Stelmachowski · G. Maniak · A. Kotarba (✉) ·  
Z. Sojka  
Faculty of Chemistry, Jagiellonian University,  
Ingardena 3, 30-060 Krakow, Poland  
e-mail: kotarba@chemia.uj.edu.pl

J.-F. Paul  
Unité de Catalyse et Chimie du Solide UMR 8181,  
Université des Sciences et Technologies de Lille,  
59655 Villeneuve d'Ascq Cedex, France

essentially based on  $\text{H}_2$ -TPR data only. Another explanation discussed the observed promotional effect of alkali in terms of the more speculative reduction of metal-oxygen bond strength which is supposed to facilitate the dioxygen desorption [11]. It was inferred from the studies on the samples deliberately doped by impregnation that even minute amounts of alkali promoter can effectively improved the catalyst performance. Once the alkali addition is further increased the beneficial effect is gradually declining. Such nonmonotonous character with the optimum at low loading may suggest that the electronic promotion is essentially responsible for the observed changes in the cobalt spinel activity in the  $\text{N}_2\text{O}$  decomposition. It is well known that adsorption of alkali promoters on metallic surfaces modifies their electronic properties gauged by the work function. Owing to the exceptionally low ionization potentials of alkali metals, a substantial part of the promotion effect is thought to be related with the charge transfer to the catalyst surface, inducing an electric field gradient at the surface, generated by the resulting dipole moment. Such effects are specially pronounced in the case of heavy alkali atoms because their large ionic radii give rise to large values of the dipole moment and the associated work function changes ( $\Delta\Phi \propto n\Delta\mu$ ) [19]. Such effect is not exclusive for metal surfaces but has been also reported for molybdenum carbide catalyst, where doping of potassium led to strongly nonmonotonous changes in the work function correlated with the analogous changes in the rate constant for indole hydrodenitrogenation [20].

In this paper we focused our attention on the elucidation of the changes in electronic properties of  $\text{Co}_3\text{O}_4$  as a function of K-loading using KOH and  $\text{K}_2\text{CO}_3$  precursors. The experimentally determined work function modifications upon potassium doping were complemented with DFT calculations and correlated with the activity of K-doped  $\text{Co}_3\text{O}_4$  catalyst in  $\text{N}_2\text{O}$  decomposition.

## 2 Experimental

The  $\text{Co}_3\text{O}_4$  samples of  $16 \text{ m}^2/\text{g}$  were obtained from commercial supplier (Fluka). Potassium doping was achieved by incipient wetness impregnation from  $\text{K}_2\text{CO}_3$  by introducing 1.2 mL of the solution with various concentrations (0.004–0.08 M) onto 1.60 g of the spinel catalyst. In the case of KOH precursor  $\text{Co}_3\text{O}_4$  samples of 250 mg were prepared by successive addition of 20  $\mu\text{L}$  portions of 0.078 M KOH, to achieved the desired K content. The potassium loading was expressed as number of atoms per  $\text{nm}^2$  ( $n_K$ ) and the corresponding samples were labelled as  $n_K\text{-K}/\text{Co}_3\text{O}_4$ . The promoted samples were next calcined at 673 K for 4 h. The BET measurements carried out by

means of a Qantasorb Junior Instrument showed no significant changes in the surface area upon doping procedure.

For the work function measurements the samples were pressed into the pellets (10 mm in diameter) under the pressure of 8 tons. Prior to work function measurements all samples were heated under primary vacuum ( $10^{-3}$  mbar) to 673 K, annealed for 15 min to decontaminate and standardize the surface. Actual measurements of the contact potential difference were performed at 423 K.

The Temperature Programmed Surface Reaction (TPSR) measurements of  $\text{N}_2\text{O}$  decomposition in the range of 293–873 K were performed in a quartz flow reactor using 500 mg of the catalyst (sieve fraction of 0.2–0.3 mm), flow rate of the feed (5%  $\text{N}_2\text{O}$ , 5%  $\text{N}_2\text{O}$  + 1%  $\text{H}_2\text{O}$  and 1,500 ppm  $\text{N}_2\text{O}$  + 1%  $\text{H}_2\text{O}$  + 3%  $\text{O}_2$  in He (5.0) feed composition were used) of  $7,000 \text{ h}^{-1}$ , and the heating rate of 10 K/min. The saturation with 1% of water was achieved by means of a thermodynamic saturator connected to a Perkin Elmer cryostat. The progress of the reaction was monitored by means of a quadrupole mass spectrometer (SRS RGA200) by following the  $m/z = 44$  ( $\text{N}_2\text{O}$ ), 32 ( $\text{O}_2$ ), 28 ( $\text{N}_2$ ), 30 ( $\text{NO}$ ), and 18 ( $\text{H}_2\text{O}$ ) lines.

The contact potential difference ( $V_{\text{CPD}}$ ) measurements were carried out by the dynamic condenser method of Kelvin with a KP6500 probe (McAllister Technical Services). The KP6500 probe was installed in vacuum chamber and the catalyst sample was mounted on a micrometric manipulator holder. The reference electrode was a standard stainless steel plate with diameter of 3 mm ( $\Phi_{\text{ref}} = 4.3 \text{ eV}$ ) provided by the manufacturer. During the measurements the gradient of the peak-to-peak versus backing potential was set to 0.2, whereas the vibration frequency and amplitude was set to 120 Hz and 40 a.u. A single  $V_{\text{CPD}}$  value was obtained using two backing potentials (reference voltages generated in preamplifier), each being an average of 20 independent measurements. The final  $V_{\text{CPD}}$  value was an average of 60 independent points. The  $V_{\text{CPD}}$  values were converted into the work function using a simple relation  $eV_{\text{CPD}} = \Phi_{\text{ref}} - \Phi_{\text{sample}}$ .

The unrestricted DFT (Density Functional Theory) calculations were performed with the Dmol<sup>3</sup> package implemented in the Materials Studio (version 2.2) of Accelrys Inc. Double-numerical quality basis set with polarization functions (DNP), semicore relativistic pseudopotentials [21, 22] and generalized gradient-corrected (GGA) functional in parameterization proposed by Perdew, Burke, and Ernzerhof (rPBE) were used in all calculations. A real-space cutoff of 4 Å was used to improve computational performance. For the Brillouin zone sampling the method proposed by Monkhorst-Pack [23], with  $2 \times 2 \times 2$  (for bulk calculations) and  $2 \times 2 \times 1$  (for slab calculations) resolution, was applied. The geometry optimization

following the BFGS scheme [24] was performed for the unit cell size and all ions position in the bulk model, and for two top layers of the slab model. Three low index (100), (110) and (111) planes of cobalt spinel were chosen for calculations with the vacuum thickness set at 10 Å. The oxide thickness was selected in such a way to ascertain comparable properties of the middle slab and the bulk atoms. Three possible models of surface potassium (potassium hydroxide, surface dissociated hydroxide and oxide species) located on the most stable (100) plane of  $\text{Co}_3\text{O}_4$  were investigated.

### 3 Results and Discussion

The typical experimental results illustrating the effect of potassium doping on  $\text{N}_2\text{O}$  decomposition efficiency is shown in Fig. 1, where the TPSR profiles are shown for bare  $\text{Co}_3\text{O}_4$  (Fig. 1b) and for the most active 1.8-K/ $\text{Co}_3\text{O}_4$  catalyst (Fig. 1a) together with the blank experiment (Fig. 1c) for dry 5%  $\text{N}_2\text{O}/\text{He}$ . The experimental data, expressed as  $\text{N}_2\text{O}$  conversion ( $X_{\text{N}_2\text{O}}$ ) versus temperature

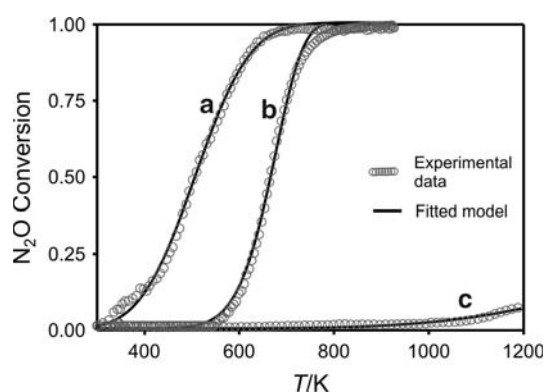


**Fig. 1** Typical TPSR results of 5%  $\text{N}_2\text{O}$  decomposition in dry atmosphere over **a** K- $\text{Co}_3\text{O}_4$  ( $K = 0.23$ ), **b** bare  $\text{Co}_3\text{O}_4$ , and **c** blank reactor. The dotted lines correspond to experimental data whereas the solid lines show the theoretical fit

( $T$ ) for the contact time  $t_s = 0.39$  s, were fitted with the kinetic model described elsewhere [25]:

$$X_{\text{N}_2\text{O}} = 1 - e^{-kt_s}$$

with the rate constant given by the Arrhenius formula  $k = A \cdot e^{-\frac{E_a}{RT}}$ , where  $E_a$ , activation energy [kJ/mol];  $R$ , gas constant [J/(mol K)]. The determined values of the activation energies and the rate constants (for  $T = 673$  K) for various feed composition and K-loading ( $n_K = 0 - 4.8$  atom  $\text{nm}^{-2}$ ) are summarized in Table 1. From comparison of the data, it can be inferred that for all samples the apparent activation barriers are lowered, whereas the corresponding rate constants are significantly increased upon K doping. The most pronounced promotional effect is observed for potassium loading in the range of  $n_K = 2 - 4$  atom  $\text{nm}^{-2}$ . In the presence of the inhibitors ( $\text{H}_2\text{O}$  and  $\text{O}_2$ ) the improvement of catalytic performance though deteriorated was still preserved, reaching 90% conversion at 703 K for the 1.8-K/ $\text{Co}_3\text{O}_4$  sample.

The activity parameters ( $E_a$  and  $T_{50\%}$  values) of the K/ $\text{Co}_3\text{O}_4$  catalysts (impregnated with  $\text{K}_2\text{CO}_3$ ) are plotted as a function of potassium loading in Fig. 2 a, b, and compared with the corresponding work function changes (Fig. 2c). All the presented curves showed nonmonotonous behavior of the  $\Phi$  values with the minimum located at  $n_K = 1.8$  atom  $\text{nm}^{-2}$ , indicating that the activity of K-doped spinel is clearly correlated with the catalyst work function. Additionally in the insert of Fig. 2c the work function variation with  $n_K$  for the catalyst obtained by impregnation with KOH is also shown. In this case the  $\Delta\Phi$  changes are less pronounced and the broader minimum is shifted towards higher loadings ( $n_K = 3.85$   $\text{nm}^{-2}$ ). Different results observed for KOH and  $\text{K}_2\text{CO}_3$  suggest that not only the alkali metal itself and its surface concentration, but also the precursor type play an important role in tuning the spinel activity. It can be explained by different nature of the resultant potassium surface species formed upon thermal pre-treatment of the samples. To substantiate this premise the changes in the work function were

**Table 1** Apparent activation energies ( $E_a$ ) and rate constants at 400 °C ( $k_{400}$ ) for  $\text{N}_2\text{O}$  decomposition over K-doped  $\text{Co}_3\text{O}_4$  catalysts for various feed compositions

Catalyst	$n_K/\text{nm}^{-2}$	$E_a/\text{kJ/mol}$			$k_{400}/\text{s}^{-1}$		
		5% $\text{N}_2\text{O}$	5% $\text{N}_2\text{O} + 1\% \text{H}_2\text{O}$	0.15% $\text{N}_2\text{O} + 1\% \text{H}_2\text{O} + 3\% \text{O}_2$	5% $\text{N}_2\text{O}$	5% $\text{N}_2\text{O} + 1\% \text{H}_2\text{O}$	0.15% $\text{N}_2\text{O} + 1\% \text{H}_2\text{O} + 3\% \text{O}_2$
$\text{Co}_3\text{O}_4$	0.00	$77.8 \pm 0.5$	$70.8 \pm 0.4$	$81.1 \pm 1.6$	1.80	0.69	0.22
	0.24	$48.6 \pm 0.5$	—	—	3.55	—	—
	0.48	$71.1 \pm 0.3$	—	—	3.72	—	—
K- $\text{Co}_3\text{O}_4$	1.83	$27.6 \pm 0.2$	$47.3 \pm 0.3$	$41.5 \pm 0.9$	8.13	4.10	4.21
	3.71	$40.9 \pm 0.3$	—	—	15.88	—	—
	4.81	$48.1 \pm 0.4$	—	—	10.76	—	—

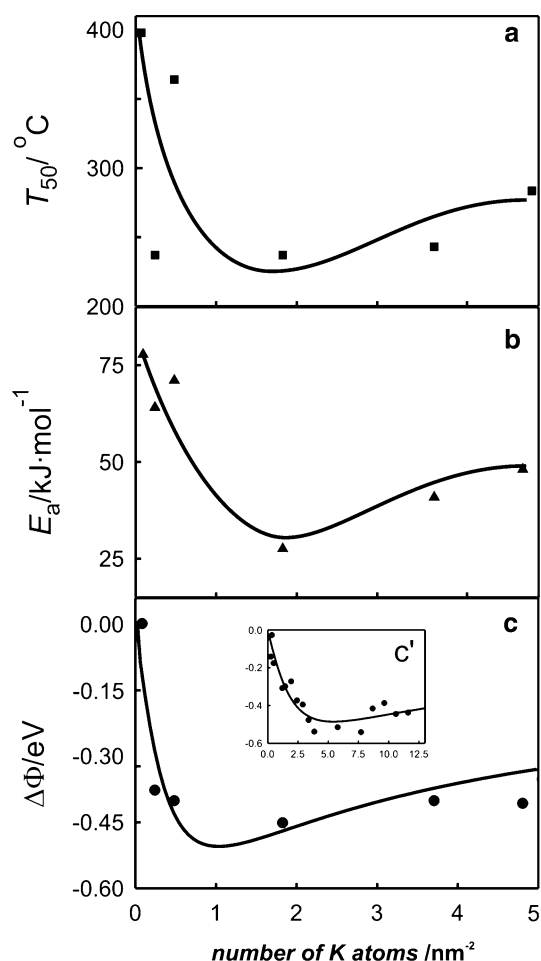


**Fig. 2** **a** The half conversion temperature of  $\text{N}_2\text{O}$  ( $T_{50\%}$ ), **b** apparent activation energy ( $E_a$ ) and **c** work function changes ( $\Delta\Phi$ ) as a function of potassium loading ( $\Theta_K$ ) introduced from  $\text{K}_2\text{CO}_3$  and (c insert) KOH precursor

analysed within the surface dipole model and corroborated by DFT calculations.

According to Helmholtz [19] at low surface loading, deposited potassium forms positive ions and associated surface dipoles giving rise to linear drop in the work function, as observed in Fig. 2c. When potassium ions come closer with the gradual increase in coverage, mutual depolarization takes place, and after passing the minimum the work function starts to increase with the amount of potassium added. The resultant nonmonotonous character of the work function variation can be analyzed in terms of the Topping equation [26]:

$$\Delta\Phi = \frac{\mu}{\epsilon_0} \cdot n_K \cdot \left( 1 + \frac{\kappa \cdot \alpha \cdot n_K^{3/2}}{4 \cdot \pi \cdot \epsilon_0} \right)^{-1},$$

where  $\Delta\Phi$  is expressed in eV,  $n_K$  in  $\text{m}^{-2}$ , and  $\kappa\alpha$  expressed in  $\text{cm}^2/\text{V}$  is the product of geometrical factor and polarizability of surface potassium. The  $\kappa$  value varies from 9 to

11 depending on the surface packing which implies that the value of polarizability of surface potassium is in the range  $\alpha = 17 - 190 \text{ \AA}$ , similar to the data for potassium adsorbed on model surfaces of transition metals [27].

Upon substitution of the numerical values the curve fitting (with *Mathematica* software) of the experimental data for the  $\text{Co}_3\text{O}_4$  samples impregnated with  $\text{K}_2\text{CO}_3$  and KOH gives effective surface dipole moment  $\mu$  equal to  $3.73 \pm 0.66$  and  $0.71 \pm 0.07 \text{ D}$ , respectively. These values confirm that the surface status of the potassium promoter is distinctly different in both cases.

This issue was further addressed by complementary DFT calculations of  $\text{Co}_3\text{O}_4$  spinel, where three models of surface potassium in the form of  $\text{KOH}_{\text{surf}}$ ,  $\text{K}_{\text{surf}}^+ + \text{OH}_{\text{surf}}^-$  and  $\text{K}_2\text{O}_{\text{surf}}$ , species were considered (vide infra). They correspond to the presumed state of the promoter deposited from hydroxide precursor upon the catalyst pre-treatment at elevated temperatures. Because of the surface state of the potassium promoter deposited from carbonate is less defined due to enhanced thermal stability of carbonates only the more clear KOH precursor case was taken for the DFT calculations.

For bulk calculations the cubic unit cell ( $a = 8.38 \text{ \AA}$ ) with 24 Co and 32 O ions was chosen [28]. The calculated and experimental geometry (Co–O distances:  $1.946\text{--}1.948 \text{ \AA}$  and  $1.1914\text{--}1.1993 \text{ \AA}$ , O–Co<sup>T</sup>–O angle:  $109.47^\circ$  and  $109.50^\circ$ ), the band gap (1.42 eV and 1.6 eV) and the magnetic state of cobalt (spin quartet for the tetrahedral and singlet for the octahedral ions) were in good agreement with available experimental data [28], indicating that the calculation scheme was selected properly. The calculated surface energies  $\gamma(100) = 1.56$ ,  $\gamma(110) = 1.90$  and  $\gamma(111) = 1.71 \text{ Jm}^{-2}$  indicate that the (100) plane is the most stable in agreement with the experiment [29, 30]. The slab model of this plane with  $\text{KOH}_{\text{surf}}$ ,  $\text{K}_{\text{surf}}^+ + \text{OH}_{\text{surf}}^-$  and  $\text{K}_2\text{O}_{\text{surf}}$  adspecies is shown in Fig. 3a–c. The  $\text{Co}_3\text{O}_4$  surface can be regarded as a series of the O–Co<sup>oct</sup>–O strips connected by alternately recessed and exposed the tetrahedral Co ions. Among several surface positions (e.g. on and between O–Co<sup>oct</sup>–O strips, next to or distant from Co<sup>T</sup>) calculated for  $\text{KOH}_{\text{surf}}$ ,  $\text{K}_{\text{surf}}^+ + \text{OH}_{\text{surf}}^-$  and  $\text{K}_2\text{O}_{\text{surf}}$  the most stable potassium species were found to be in hollow positions between tetrahedral cobalt ions. The energy of potassium in such a hollow position is lower by 30 kcal/mol. This localization is also favourable from the view point of oxygen recombination. Decomposition of  $\text{N}_2\text{O}$  over cobalt spinel can be analysed within the three-step mechanism: activation by abstraction of the oxygen atom ( $\text{N}_2\text{O} \rightarrow \text{N}_2 + \text{O}_{\text{surf}}$ ), surface diffusion of oxygen adatoms and their recombination into dioxygen molecule [8, 31, 32]. It has been recently shown that recombination of the oxygen atoms via surface diffusion occurs through the cationic and ionic sites along the O–Co<sup>oct</sup>–O strips (Fig. 3).



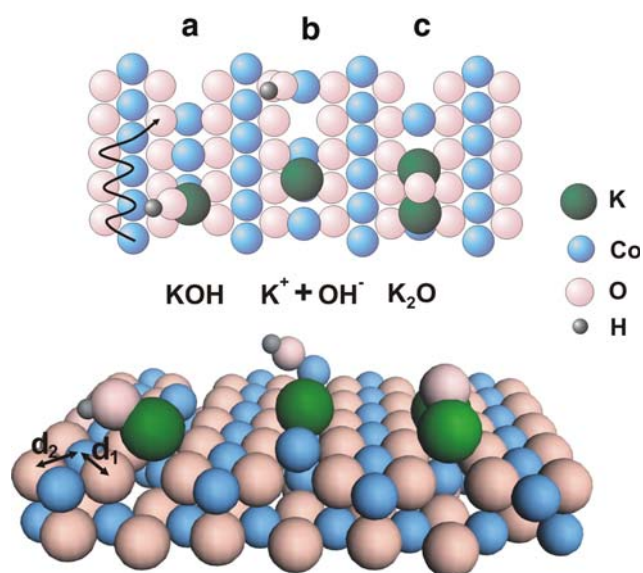


**Fig. 3** The model of  $\text{Co}_3\text{O}_4$  spinel structure with exposed (100) surface. Three most stable potassium adsorption modes: **a** potassium hydroxide, **b** dissociated potassium hydroxide and **c** potassium oxide

This process by involving  $\text{O}^-$ ,  $\text{O}$ , and  $\text{O}_2^{2-}$  intermediates is accompanied by the consecutive changes in the oxidation state of the diffusing oxygen adatom [31]. Thus, having a pronounced redox character the recombination process strongly depends on the electronic properties of the catalyst. Indeed, as shown in Fig. 2 by appropriate potassium doping the chemical potential of electrons of the catalyst can be tuned for optimal performance in the implicated redox cycles.

The DFT calculations allowed for an insight into the changes in the Hirshfeld charges and in interatomic bond lengths in  $\text{KOH}_{\text{surf}}$ ,  $\text{K}^+_{\text{surf}} + \text{OH}^-_{\text{surf}}$  and  $\text{K}_2\text{O}_{\text{surf}}$  induced upon adsorption. The changes in total atomic charge of +0.25, +0.28 and +0.59 for  $\text{KOH}_{\text{surf}}$ ,  $\text{K}^+_{\text{surf}} + \text{OH}^-_{\text{surf}}$  and  $\text{K}_2\text{O}_{\text{surf}}$ , respectively, were observed, indicating significant electron density donation towards the  $\text{Co}_3\text{O}_4$  spinel. The most pronounced modification in charge distribution in all potassium adspecies were observed on the oxygen moiety, with  $\Delta q = 0.27$ , 0.30 and 0.40 for  $\text{KOH}_{\text{surf}}$ ,  $\text{K}^+_{\text{surf}} + \text{OH}^-_{\text{surf}}$  and  $\text{K}_2\text{O}_{\text{surf}}$ , respectively. Electron density transfer to the surface was distributed mainly to adjacent surfaces oxygen atoms (four in the case of  $\text{KOH}$ , and six for  $\text{K}_2\text{O}$ , see Fig. 3) and the nearest octahedral cobalt ions. Both adsorbed  $\text{KOH}_{\text{surf}}$  and  $\text{K}_2\text{O}_{\text{surf}}$  species become strongly bend ( $\angle \text{K-O-H} = 113^\circ$ , and  $\angle \text{K-O-K} = 109^\circ$ ) in comparison to isolated linear stable structures. The bond length between potassium and surface oxygen was found to be 2.20 for  $\text{KOH}$  and 2.25 Å for  $\text{K}_2\text{O}$ . The slight changes in Co-O surface distances were also caused by potassium doping of  $\text{Co}_3\text{O}_4$ . As a result oxygen ions in the vicinity of the adspecies are displaced towards potassium, which leads

to the lengthening of  $d_1$  distance between  $\text{Co}^{\text{oct}}$  and  $\text{O}^{2-}(\text{K})$  (from 1.915 to 1.926 Å) and simultaneous shortening of the distance  $d_2$  between octahedral cobalt and the opposite  $\text{O}^{2-}$  (from 1.915 to 1.901 Å) (Fig. 3). In the case of dissociative  $\text{K}^+_{\text{surf}} + \text{OH}^-_{\text{surf}}$  adsorption mode the resultant hydroxyl group can be localized on  $\text{Co}^{\text{tet}}$  and  $\text{Co}^{\text{oct}}$  sites with the energy lower than for undissociative  $\text{KOH}$  of 21.4 and 11.2 kcal/mol, respectively. The potassium moiety with an atomic charge of +0.53(5) is situated perpendicularly above the surface oxygen at a distance of 2.14 Å.

Using the Hirshfeld atomic charge and the calculated distances and neglecting the intratomic charge polarization the resultant electric dipole moments for all the potassium adspecies were calculated from the formula  $\mu_n = \sum q_i r_{i,n}$ , where  $q_i$  and  $r_{i,n}$  are the Hirshfeld charge and the  $n$ -th coordinate of atom  $i$ , respectively [33]. The calculated dipole moments were found to be  $\mu_{\text{KOH}} = 0.44$  D,  $\mu_{\text{K}_2\text{O}} = 1.25$  D and for bare potassium in the dissociative mode  $\mu_{\text{K}^+_{\text{surf}}} = 1.4(5)$  D. In the latter case inclusion of the adjacent  $\text{OH}^-_{\text{surf}}$  group reduced the resultant dipole moment to 1.1(2) D. The correlation between calculated values are in reasonable agreement with the corresponding average experimental value of  $\mu_{\text{KOH}} = 0.7$  D, derived from Topping analysis of the work function changes with potassium loading in accordance with the electronic nature of the promotional effect of adsorbed K species.

## 4 Conclusions

The experimental and theoretical results obtained for the K-doped  $\text{Co}_3\text{O}_4$  spinel revealed that the beneficial effect of potassium doping is associated with the work function lowering of the catalyst (reaching  $\Delta\Phi = 0.5$  eV in the optimal case). This facilitates the redox processes occurring between the catalyst surface and the reaction intermediates produced during the  $\text{N}_2\text{O}$  decomposition. As a result at the optimal potassium loading (1.8 atoms/ $\text{nm}^2$ ), the apparent activation energy for  $\text{N}_2\text{O}$  decomposition could be lowered from 78 to 28 kJ/mol, whereas the temperature of half conversion decreased by 100 K upon the impregnation with potassium carbonate.

**Acknowledgments** This work was done within The European Research Project COST D41.

## References

1. Pérez-Ramírez J, Kapteijn F, Schöffel K, Moulijn JA (2003) Appl Catal B 44:117
2. Kondratenko EV, Pérez-Ramírez J (2007) Catal Today 121:197
3. Kapteijn F, Rodríguez-Mirasol J, Moulijn JA (1996) Appl Catal B 9:25

4. Lunsford JH (1975) *The Catalytic Chemistry of Nitrogen Oxides*. Plenum, New York
5. Haber J, Machej T, Janas J, Nattich M (2004) *Catal Today* 90:15
6. Haber J, Nattich M, Machej T (2008) *Appl Catal B* 77:278
7. Russo N, Mescia D, Fino D, Saracco G, Speccia V (2007) *Ind Eng Chem Res* 46:4226
8. Obalona L, Fila V (2007) *Appl Catal B* 70:353
9. Abu-Zied BM, Schwieger W, Unger A (2008) *Appl Catal B*. doi: [10.1016/j.apcatb.2008.04.004](https://doi.org/10.1016/j.apcatb.2008.04.004)
10. Kondratenko EV, Kondratenko VA, Santiago M, Perez-Ramírez J (2008) *J Catal* 256:248
11. Haneda M, Kintaichi Y, Bion N, Hamada H (2003) *Appl Catal B* 46:473
12. Asano K, Ohnishi C, Iwamoto S, Shioya Y, Inoue M (2008) *Appl Catal B* 78:242
13. Ohnishi C, Asano K, Iwamoto S, Chikama K, Inoue M (2007) *Catal Today* 120:145
14. Omata K, Takada T, Kasahara S, Yamada M (1996) *Appl Catal A* 146:255
15. Yan L, Ren T, Wang X, Ji D, Suo J (2003) *Appl Catal B* 45:85
16. Yan L, Ren T, Wang X, Gao Q, Ji D, Suo J (2003) *Catal Commun* 4:505
17. Liotta LF, Di Carlo G, Pantaleo G, Deganello G (2005) *Catal Commun* 6:329
18. Xue L, Zhang C, He H, Teraoka Y (2007) *Catal Today* 126:449
19. Somorjai GA (1994) *Introduction to Surface Chemistry and Catalysis*. New York, Wiley
20. Kotarba A, Adamski G, Piskorz W, Sojka Z, Sayag C, Djega-Mariadassou GJ (2004) *Phys Chem B* 108:2885
21. Benedek NA, Snook IK, Latham K, Yarovsky IJ (2005) *J Chem Phys* 122:144102
22. DMol3 User Guide (2003) Accelrys Inc., San Diego, CA
23. Monkhorst HJ, Pack JD (1976) *Phys Rev B* 13:5188
24. Fisher TH, Almlof J (1992) *J Phys Chem* 96:9768
25. Chang KS, Song H, Park Y-S, Woo J-W (2004) *Appl Catal A: General* 273:223
26. Brison J, Mine N (2007) *Surf Sci* 601:1467
27. Verhoef RW, Asscher M (1997) *Surf Sci* 391:11
28. Wang L, Maxish T, Ceder G (2006) *Phys Rev B* 73:195107
29. Tang X, Li J, Hao J (2007) *Mater Res Bull.* doi: [10.1016/j.materresbull.2007.12.009](https://doi.org/10.1016/j.materresbull.2007.12.009)
30. Xu R, Chun-Zeng H (2003) *J Phys Chem B* 107:926
31. Piskorz W, Zasada F, Stelmachowski P, Kotarba A, Sojka Z (2008) *Catal Today* 137:418
32. Scagnelli A, Valentin CD, Pacchioni G (2006) *Surf Sci* 600:386
33. De Proft F, Van Alsenoy C, Peeters A, Langenaeker W, Geerlings P (2002) *J Comput Chem* 23:1198